

# Supplementary Materials for

The Sun's Role for Decadal Climate Predictability in the North Atlantic

Annika Drews<sup>1,2</sup>, Wenjuan Huo<sup>1</sup>, Katja Matthes<sup>1</sup>, Kunihiro Kodera<sup>3,4</sup>, and Tim Kruschke<sup>5</sup>

**This PDF file includes:**

Extended figures and tables.

Figs. S1 to S9

Table S1

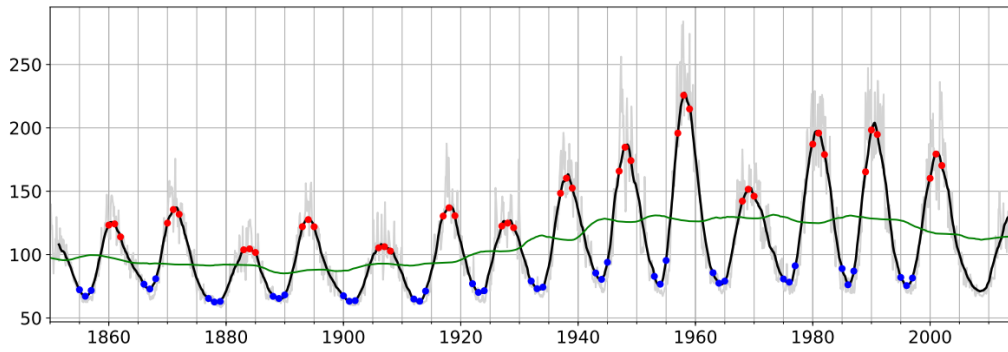


**Fig. S1. Solar cycle-based composite definition.** Monthly (thin grey line) and 3-year running mean of the solar radio flux at 10.7 cm in solar flux units ( $1 \text{ sfu} = 10^{-22} \text{ Wm}^{-2} \text{ Hz}^{-1}$ ) for the FULL experiment (orange line) and LOWFREQ (green line). Red (blue) dots indicate the solar maximum (minimum) indices used for solar cycle-based composites.

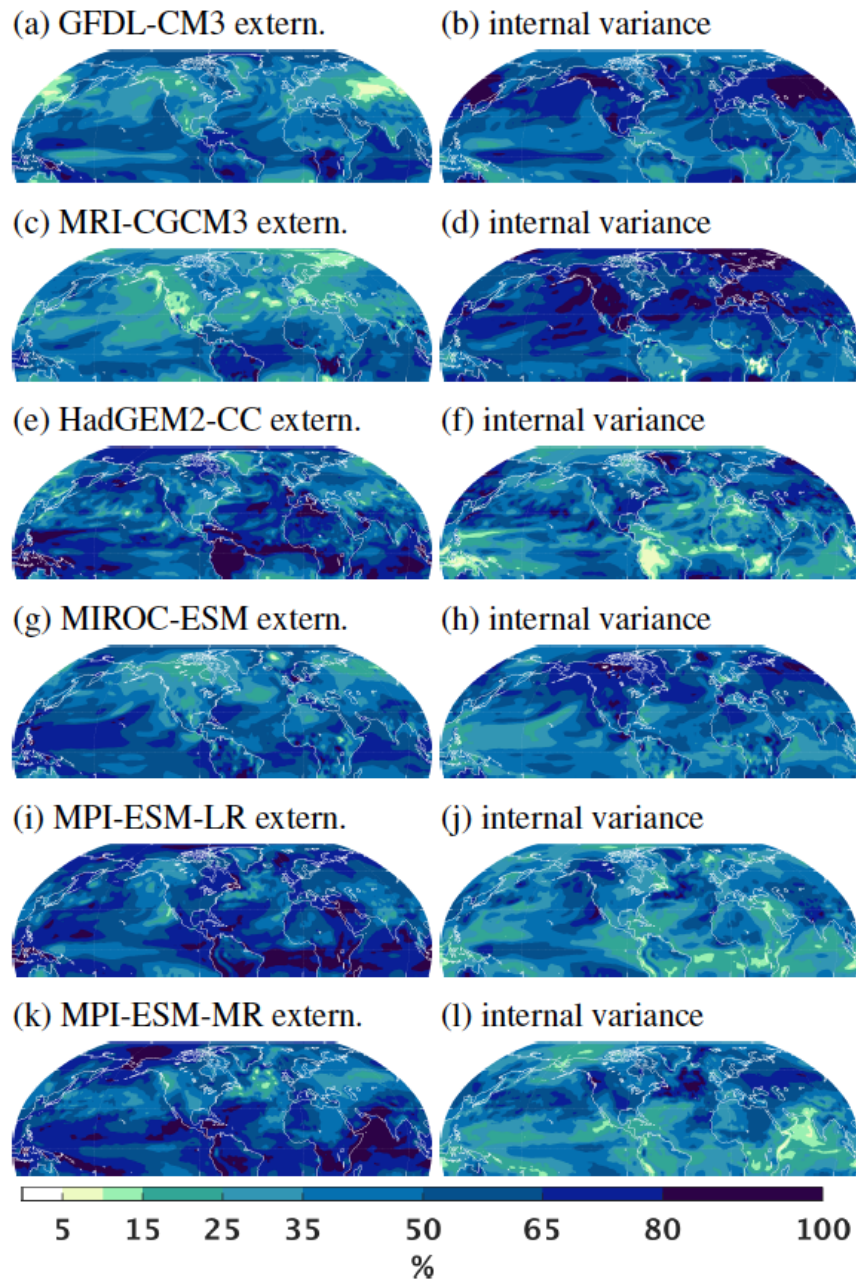


**Fig. S2. Decadal potential predictability due to the external forcings and internal climate variability.** Potential predictability variance fraction (explained variance) with respect to DJF averaged surface air temperature and associated with all external forcings (including full solar forcing) (left column), and remaining variance fraction due to internal climate variability (right column) in 6 CMIP5 high-top models.

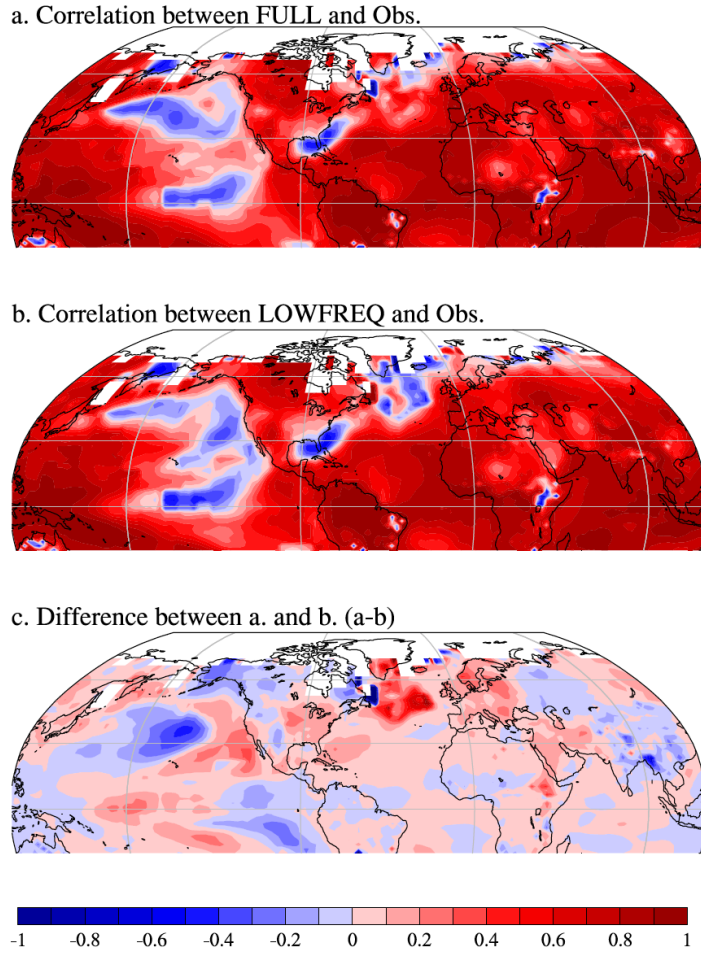


**Fig. S3. Quantification of the forecast skill of climate predictions.** a. Correlation coefficients of DJF averaged surface air temperatures between observations (NOAAGlobeTemp) and the FULL ensemble mean during the strong epoch. b. Same as a., but for observations and LOWFREQ ensemble mean. c. Correlation differences between a. and b. Note that there are large differences, shown in c, of the correlations between observations and FULL (a) compared to the correlation of observations and LOWFREQ (b) in the North Atlantic. This typical deterministic measure indicates a gain in skill when the solar cycle is added to the model.

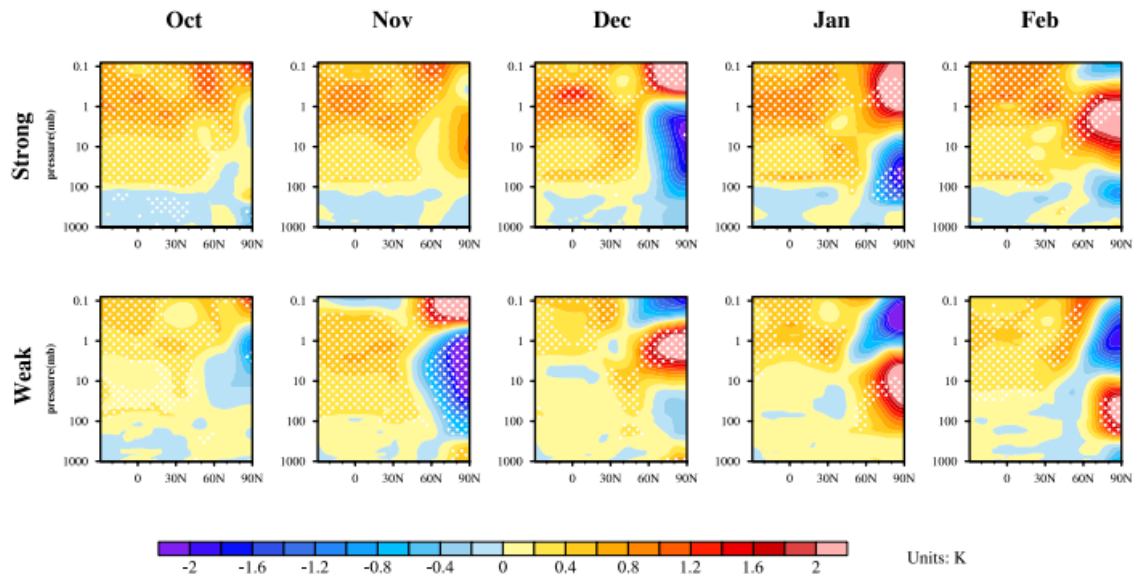


**Fig. S4. Solar cycle response in zonal mean temperatures during the strong (top) and weak (bottom) epoch.** Latitude-height cross sections from 30°S to 90°N and 1000 hPa to 0.1 hPa of solar-cycle based composite differences (in K) at lag 0. Significance levels are indicated by white dots (90%) based on a 1000-fold bootstrapping test. See “Methods” section for more details.

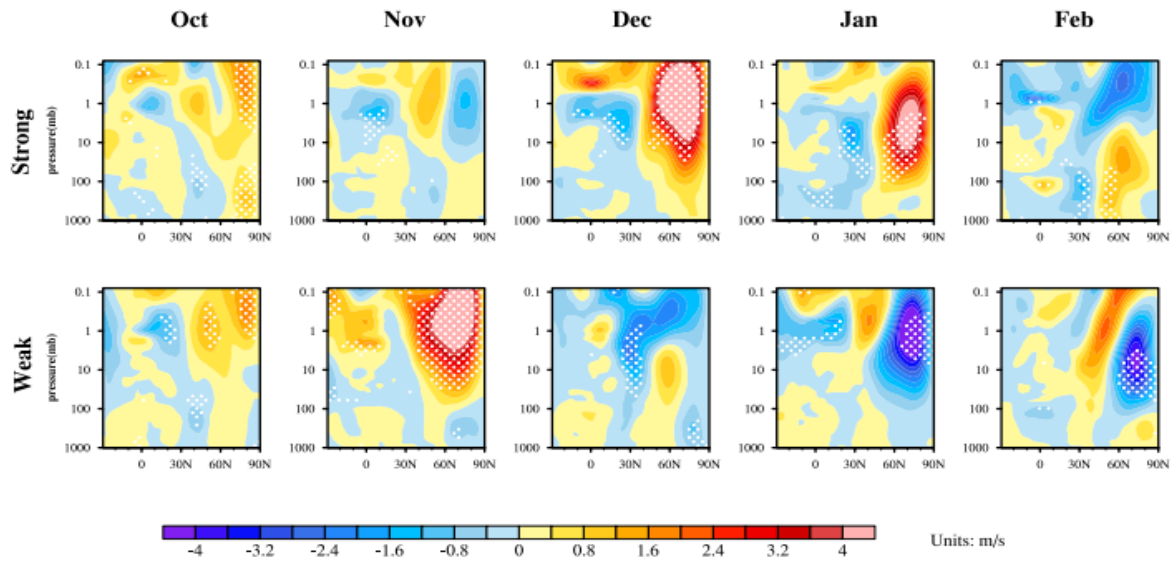


**Fig. S5. Solar cycle response in zonal mean zonal winds during the strong (top) and weak (bottom) epoch.** Latitude-height cross sections from 30°S to 90°N and 1000 hPa to 0.1 hPa of solar-cycle based composite differences (in m/s) at lag 0. Significance levels are indicated by white dots (90%) based on 1000-fold bootstrapping test. See “Methods” section for more details.

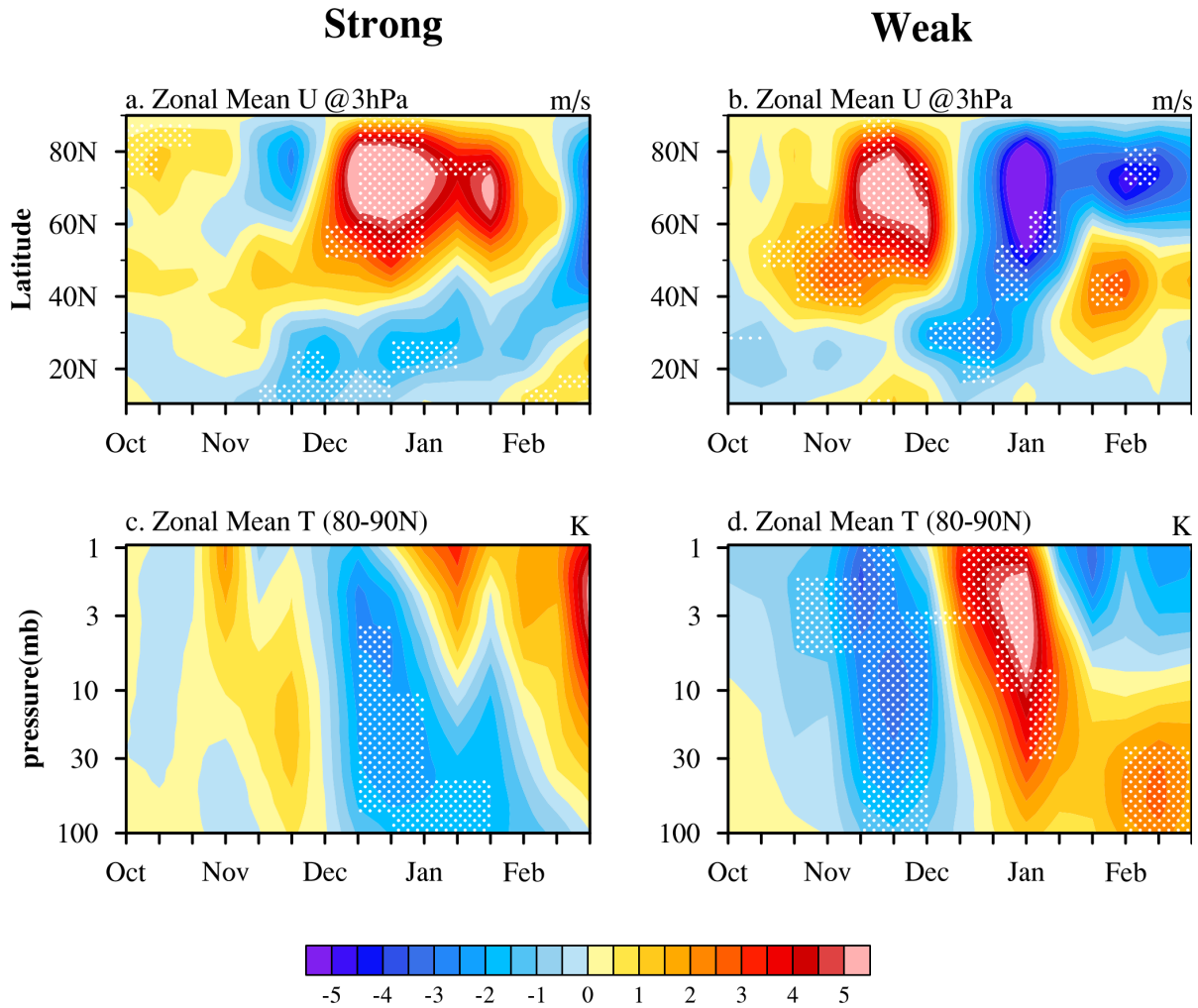


**Fig. S6. Seasonal march of the solar signal in zonal mean zonal winds and zonal mean temperature during the strong (left) and weak (right) epoch.** (a-b) Time-latitude cross sections of solar-cycle based composite differences of 10-day means in zonal mean zonal wind (in m/s) around 3hPa at lag 0; (c-d) Time-height cross sections from October through February and 100 hPa to 1 hPa of solar-cycle based composite differences of 10-day means in zonal temperature averaged over the polar cap(80-90N) (in K) at lag 0. Significance levels are indicated by white dots (90%) based on a 1000-fold bootstrapping test. See “Methods” section for more details.

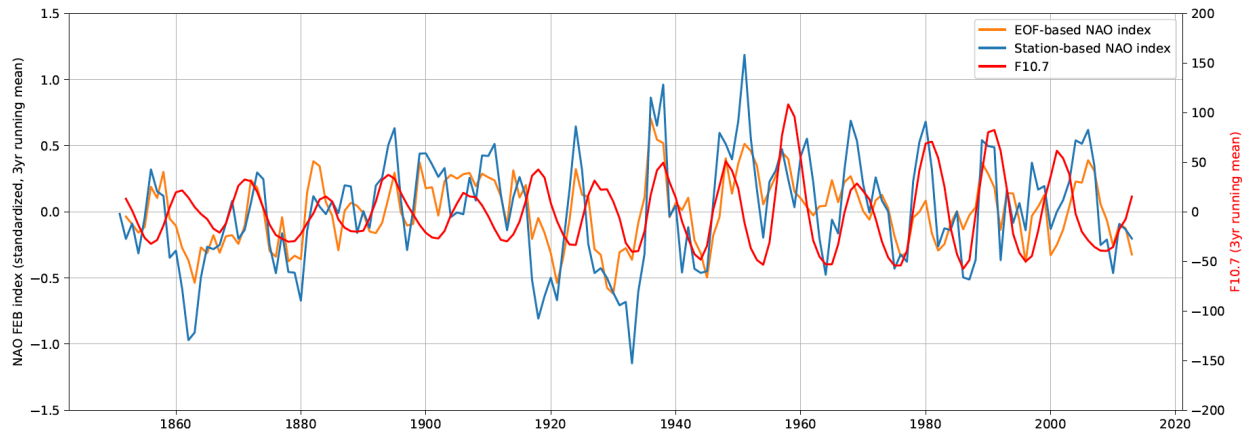


**Fig. S7. Correlations between the 11-year solar cycle and two different NAO indices from the model simulations.** The F10.7 (red), ensemble mean of EOF-based NAO index (orange) and the station-based NAO-like index (blue), both time series have been smoothed with a 3-year running mean.



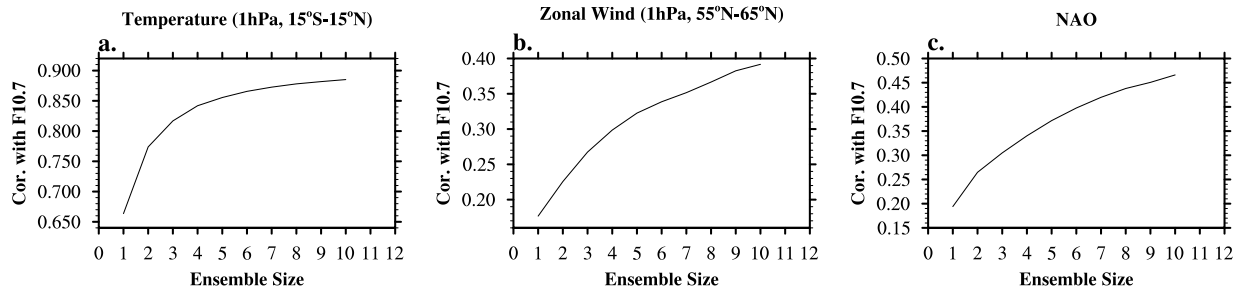


**Fig. S8. Dependence of “detectability” of isolated solar signals on the number of ensemble members.** Correlation with F10.7 as a function of ensemble size for a. December tropical stratopause temperature (1hPa, 15°S-15°N); b. December zonal mean zonal wind (1hPa, 55°N-65°N); and c. NAO index. For these figures, we randomly sampled subsets of the simulations from the 10 members and calculated the correlation of the solar signal in these subsets with the solar index 100 times.

## SLP (HadSLP2) in Feb.

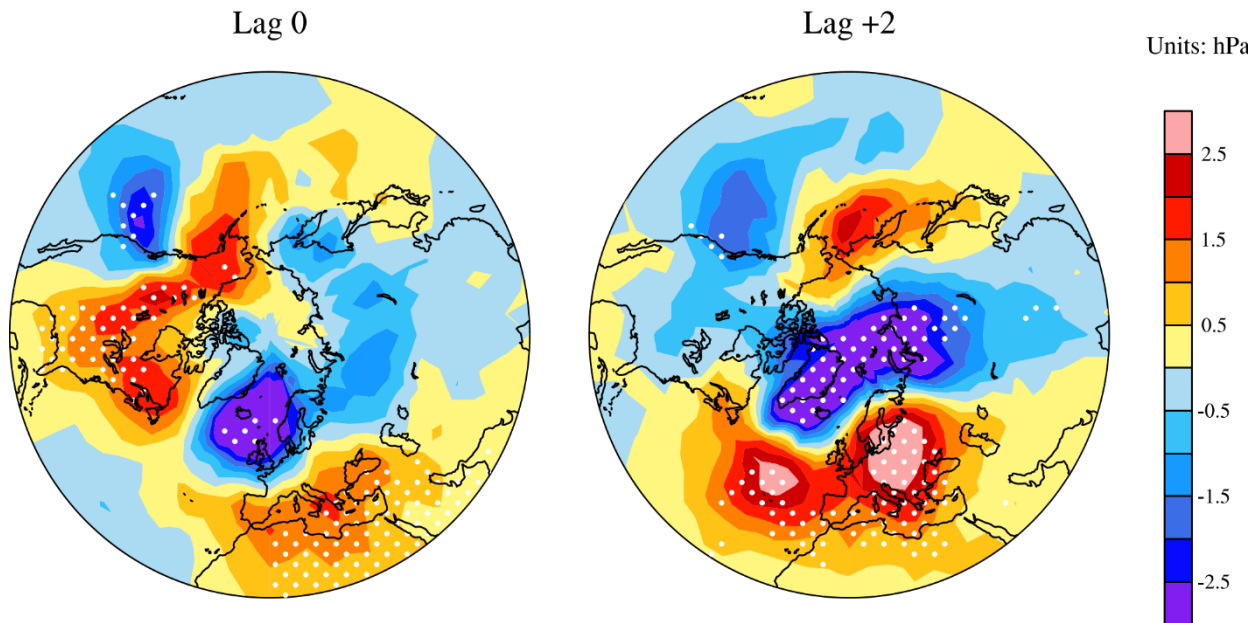


**Fig. S9. Comparison of solar-induced SLP anomalies in the model vs. observations.** Lagged composite differences of solar maximum minus minimum for observed SLP (HadSLP2) anomalies in February during the strong epoch at lag 0 (left) and lag +2 (right) years. Note that the observed signal includes the full solar signal (i.e. the solar cycle as well as the low-frequency part of the solar signal) and internal variability. White dots indicate the 90% statistical significance level based on 1000-fold bootstrapping test.

**Table S1.**

Amplitudes of solar cycles in the weak and strong epochs, indicated by F10.7cm

Weak Epoch	Solar cycle	10	11	12	13	14	15	16
	Amplitude (Max-Min)	53.9	53.6	45.6	57.4	41.4	72.4	55.2
	Standard deviation	18.3	23.8	16.7	22.9	19.4	26.8	25.0
Strong Epoch	Solar cycle	17	18	19	20	21	22	23
	Amplitude (Max-Min)	89.8	99.2	161.7	81.5	124.8	137.8	111.6
	Standard deviation	31.7	37.4	60.4	32.5	48.1	54.1	38.8